

# Historical harvests reduce neighboring old-growth basal area across a forest landscape

DAVID M. BELL,<sup>1,3</sup> THOMAS A. SPIES,<sup>1</sup> AND ROBERT PABST<sup>2</sup>

<sup>1</sup>USDA Forest Service Pacific Northwest Research Station, 3200 SW Jefferson Way, Corvallis, Oregon 97331 USA

<sup>2</sup>Department of Forest Ecosystems and Society, Oregon State University, 321 Richardson Hall, Corvallis, Oregon 97331 USA

**Abstract.** While advances in remote sensing have made stand, landscape, and regional assessments of the direct impacts of disturbance on forests quite common, the edge influence of timber harvesting on the structure of neighboring unharvested forests has not been examined extensively. In this study, we examine the impact of historical timber harvests on basal area patterns of neighboring old-growth forests to assess the magnitude and scale of harvest edge influence in a forest landscape of western Oregon, USA. We used lidar data and forest plot measurements to construct 30-m resolution live tree basal area maps in lower and middle elevation mature and old-growth forests. We assessed how edge influence on total, upper canopy, and lower canopy basal area varied across this forest landscape as a function of harvest characteristics (i.e., harvest size and age) and topographic conditions in the unharvested area. Upper canopy, lower canopy, and total basal area increased with distance from harvest edge and elevation. Forests within 75 m of harvest edges (20% of unharvested forests) had 4% to 6% less live tree basal area compared with forest interiors. An interaction between distance from harvest edge and elevation indicated that elevation altered edge influence in this landscape. We observed a positive edge influence at low elevations (<800 m) and a negative edge influence at moderate to high elevations (>800 m). Surprisingly, we found no or weak effects of harvest age (13–60 yr) and harvest area (0.2–110 ha) on surrounding unharvested forest basal area, implying that edge influence was relatively insensitive to the scale of disturbance and multi-decadal recovery processes. Our study indicates that the edge influence of past clearcutting on the structure of neighboring uncut old-growth forests is widespread and persistent. These indirect and diffuse legacies of historical timber harvests complicate forest management decision-making in old-growth forest landscapes by broadening the traditional view of stand boundaries. Furthermore, the consequences of forest harvesting may reach across ownership boundaries, highlighting complex governance issues surrounding landscape management of old-growth forests.

*Key words:* basal area; disturbance legacies; edge influence; lidar; old-growth forest; timber harvesting.

## INTRODUCTION

Forest disturbances, such as timber harvesting, can have large effects on ecosystem structure and function (Franklin et al. 2002, Turner 2010) and neighboring undisturbed forests (Harper et al. 2005). For example, clearcutting in Oregon and Washington (hereafter, the Pacific Northwest, USA) during the 20th century has not only reduced the area of old-growth and mature forest (Davis et al. 2015), but altered the microenvironment and structure of unharvested forests adjacent to harvest units (Chen et al. 1993, 1995) while increasing the amount of edge habitat in the landscape (Spies et al. 1994). Clearcutting can alter the understory microenvironment in a neighboring old-growth forest at distances of tens to hundreds of meters into the intact old-growth forest (Chen et al. 1993, 1995, Harper et al. 2005, 2015, Esseen et al. 2016). The distance of microclimate

impacts from clearcut patches can exceed those of smaller canopy gaps, which are part of natural successional processes, by a factor of five or more (Gray et al. 2002). These impacts on microenvironment are likely to alter ecosystem function and structure (Chen et al. 1999). For example, tree growth, density of dead trees, and density of tree seedlings all increased near harvest edges in an old-growth *Pseudotsuga menziesii* and *Tsuga heterophylla* forest neighboring a 50-yr-old, 96-ha clearcut (Chen et al. 1992). Because most studies of edge influence associated with clearcutting have focused on a few sites, our understanding of the frequency and magnitude of edge influence on vegetation structure and composition at landscapes scales is limited.

Applying existing field-based results to landscape assessment of ecological processes and patterns are limited by the cost of implementing large, well-replicated experiments across controls (e.g., forest interiors) and treatments (e.g., forest edges) (Hurlbert 1984, Oksanen 2001). The large sample sizes needed to assess the edge influence of timber harvests across entire landscapes make field-based methods impractical (but see Esseen

Manuscript received 20 September 2016; revised 16 March 2017; accepted 27 March 2017. Corresponding Editor: Emil Cienciala.

<sup>3</sup>E-mail: dmbell@fs.fed.us

et al. 2016). Advances in remote sensing have made stand, landscape, and regional assessments of the direct impacts of disturbance on forests quite common (e.g.; Kennedy et al. 2012, Davis et al. 2015) and in some cases these methods can contribute to our understanding of the edge influence by disturbance. Spies et al. (1994) estimated edge influence of clear cutting in the western Oregon Cascade Mountains using Thematic Mapper (TM) imagery and assuming a fixed 100 m width of edge influence (general effects including microclimate and forest structure) into closed canopy conifer forests from adjacent cutting units. They found that this type of edge in the landscape increased from about 9.5% to over 13% between 1972 and 1988 but they were not able to measure the edge influence on forest structure directly. The advent of high resolution, active, remote sensing techniques capable of characterizing the horizontal and vertical distribution of vegetation, such as airborne light detection and ranging (lidar), has made more refined assessments of forest structure possible. Lidar can estimate many facets of forest structure across forest landscapes, including tree basal area and biomass (Seidl et al. 2012, Zald et al. 2016), snag density (Wing et al. 2014), characteristics of individual trees (Andersen et al. 2014), and habitat quality for wildlife (Ackers et al. 2015). The increasing availability of lidar data offers an opportunity to directly measure the magnitude and scale of edge influence on forest structure across large areas.

Timber harvesting edge influence on unharvested forest structure is complex, involving multiple ecological processes, such as tree growth and mortality, which vary in space and time. Upper canopy (i.e., exposed to open sky) and lower canopy (i.e., shaded by larger trees) components of forest structure might respond differently to nearby forest harvest, with understory tree biomass responding positively to increased resource availability (Canham 1988, Clark et al. 2012) and overstory tree biomass responding negatively as a result of increased mortality, the latter probably associated with greater chance of windthrow (Huggard et al. 1999). Most evidence suggests that edge influence is more pronounced and extend further into the overstory compared to understory, though the magnitude is also influenced by local factors such as aspect, edge abruptness, density of the forest, patch contrast in canopy height, and disturbance history (Harper et al. 2005, Esseen et al. 2016). In addition, characteristics of the harvest itself, such as clearcut size, presence and distribution of remnant trees, and time since harvest, will affect the mitigation of edge influence (i.e., diminishing edge influence through time).

In this work, we examine the impact of historical timber harvests on basal area patterns of neighboring old-growth forests to assess the magnitude and scale of harvest edge influence in a forest landscape of western Oregon, USA. Our objectives were to (1) quantify edge influence for clearcut units of differing ages and sizes and (2) assess differences in edge influence on basal area between upper canopy and lower canopy tree communities. We used lidar

data and forest plot measurements to construct 30-m resolution maps of total, upper canopy, and lower canopy tree basal area in lower and middle elevation mature and old-growth forests within the H. J. Andrews Experimental Forest. We then assessed how edge influence on total, upper canopy, and lower canopy basal area varies across this forest landscape as a function of harvest characteristics (i.e., harvest size and age) and topographic conditions in the unharvested area. By integrating field observations and remote sensing for examining the impacts of historical forest harvests on neighboring unharvested forest, this work provides a framework for mapping complex forest structural variation essential for forest landscape management and monitoring.

## METHODS

### *Study area and data*

This research was carried out at the 6,400-ha H. J. Andrews Experimental Forest (HJA) located in the Cascade Mountains of western Oregon, USA (44.2° N, 122.2° W). Established in 1948, HJA has played a key role in basic and applied forest ecosystem research in the Pacific Northwest (Luoma 2006). The HJA covers elevations from 410 to 1,630 m (Fig. 1a), with forests dominated by *Pseudotsuga menziesii*, *Tsuga heterophylla*, and *Thuja plicata* at low elevations and forests dominated by *Abies procera*, *Abies amabilis*, *P. menziesii*, and *T. heterophylla* at high elevations. Harvesting in the HJA began in 1950 and continued until the mid-1980s, roughly a decade prior to cessation of most timber harvesting activities on national forest lands associated with the Northwest Forest Plan (Davis et al. 2015). Harvest patches in the HJA range from 13 to 60 yr in age and 0.2 to 119.0 ha in size (Fig. 1b).

We identified 102 circular, 17.84 m radius tree plots distributed across three unharvested watersheds at HJA measured in 2008 and 2009 that were appropriate for characterizing forest structure with lidar data. Mean total basal area, upper canopy basal area, and lower canopy basal areas were  $76.0 \pm 25.8$  m<sup>2</sup>/ha (mean  $\pm$  SD),  $63.4 \pm 25.1$  m<sup>2</sup>/ha, and  $12.5 \pm 6.7$  m<sup>2</sup>/ha, respectively. Canopy heights (here described by 95th percentile height of lidar first returns greater than 1 meter above the ground within 25-m<sup>2</sup> cells) of forests ranged from 0 to 95 m, with the most dramatic transitions in canopy height occurring across the boundary between harvested and unharvested forests (Fig. 2). All three watersheds, and much of the unharvested forest within the study area, are at least 200 yr old, originating after stand-replacing fires. The tree plots share common measurement methodologies and were likely sufficiently large (approximately 900 m<sup>2</sup> area after slope correction) to minimize issues associated with plot boundaries and co-registration errors in lidar-based estimation of tree basal area (Frazer et al. 2011). At each plot, trees were measured for diameter, among other things (for plot details regarding plot establishment, see Chen et al. [1992]), and classified by canopy status

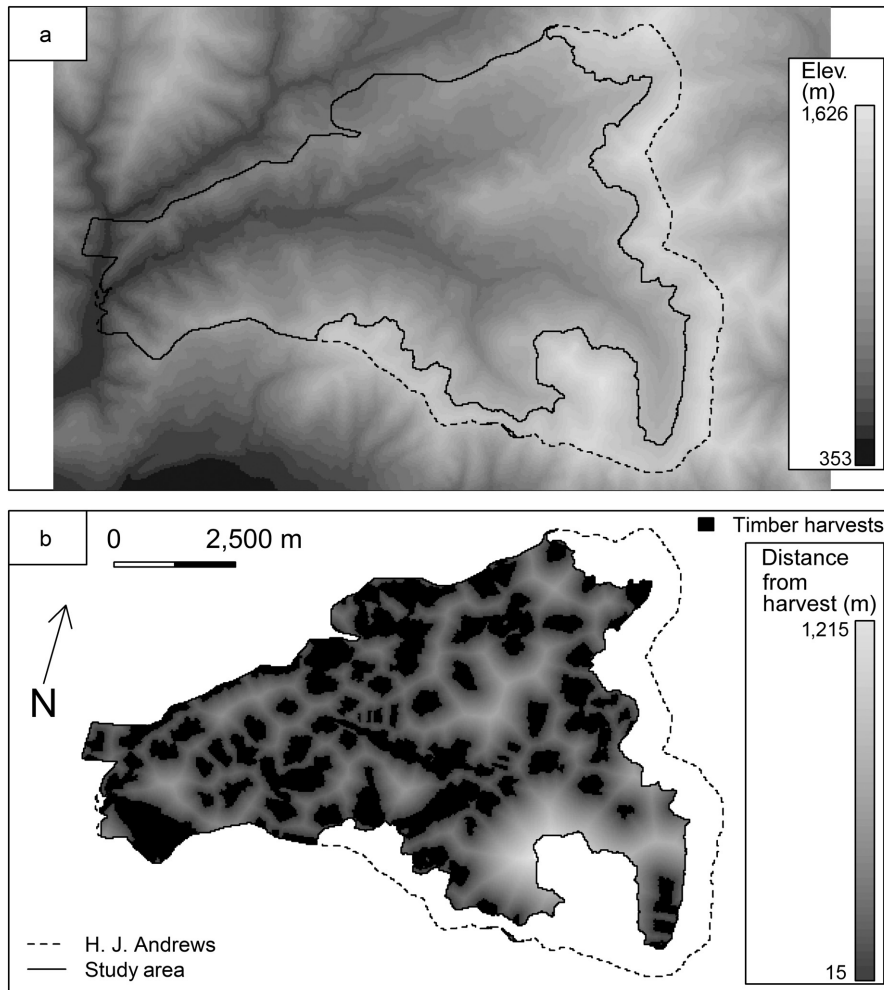


FIG. 1. Map of (a) elevation and (b) distance from timber harvests in our study area.

(dominant, codominant, intermediate, and suppressed) based on visual inspection (e.g., Latifi et al. 2016). Examination of diameter data indicated that these canopy classes correlated with tree size. Trees were grouped based on canopy status as upper canopy trees (dominant and codominant) and lower canopy trees (intermediate and suppressed) and plot basal area per unit area ( $\text{m}^2/\text{ha}$ ) was calculated. The upper and lower canopy groups roughly correspond to trees that are directly observed by aerial remote sensing (i.e., exposed canopies) and trees that are obscured from view by larger trees, thus providing less direct information about tree structure. Because elevations of the tree plots ranged from 476 to 1,177 m, we limited the study to elevations within 50 m of this range (i.e., 426 to 1,227 m; Fig. 1a).

Lidar remote sensing of forest canopy structure at HJA has been ongoing since the 1990s (Lefsky et al. 1999), with an August 2008 acquisition supporting improved mapping of forest biomass at the HJA (Seidl et al. 2012, Zald et al. 2016). Technical details of the data acquisition are provided in Appendix S1. To represent vertical

structure in the forest canopy, we extracted the proportion of the total lidar returns for each 5-m height bin to represent the canopy height profile for (1) topographically corrected plot footprints and (2) a grid of 30-m pixels covering the study area (Fig. 1) matching Landsat-based vegetation products used in a previous study of landscape forest dynamics in HJA (Seidl et al. 2012). Given that average pulse return density was 9 points/ $\text{m}^2$ , each 30-m pixel averaged 8,100 points per pixel upon which height profiles could be based.

To avoid multicollinearity while still representing the complex variation in lidar data reflective of forest structure, we performed a principal component analysis on the canopy height profile data for all unharvested 30-m pixels in the study area. This approach helps to minimize the correlations between covariates in the lidar data whilst retaining major types of variation represented in the lidar data (Finley et al. 2013). Lidar data from harvested areas were avoided to maximize the information in the principal components analysis relative to unharvested forest structure. Harvest boundaries were based

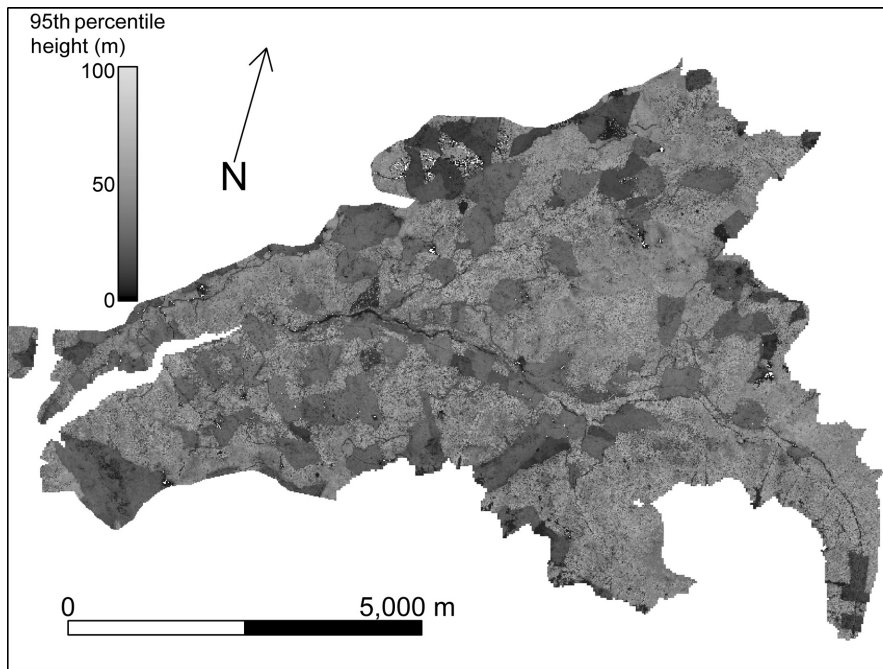


FIG. 2. Canopy height (m; 95th percentile) for lidar first returns more than 1 meter above the ground within 5-m footprints.

on harvest maps created using historical aerial photographs that were later corrected for image distortion and spatial registration errors (Zald et al. 2016). Corrections involved manual retracing of harvest boundaries based on 95th percentile vegetation height from the 2008 lidar data acquisition. Thus, harvest boundaries were defined as the transition in canopy architecture from tall, remnant trees in uncut stands to shorter tree and shrub regrowth within harvest units. For assessing the influence of harvest edges on basal area in uncut forest (see *Assessing edge influence*), we excluded 30-m pixels within 15 m of this harvest boundary to avoid the mixing of uncut and harvested vegetation.

The first four axes of the principal component analysis explained 85.2% of the variation in the canopy height profile data (Fig. 3). Axis 1 differentiated between tall, closed-canopy forests (returns above 35 m) and short-stature and/or open forest (returns below 20 m). Axis 2 differentiated between closed-canopy, moderate height forests (20–40 m) and tall forest (>45 m) with understory or bare earth (<10 m). Axis 3 differentiated between moderate height forest (30–40 m) with understory or bare-earth returns (<10 m) and tall forest (>50 m) with a second sub-canopy cohort of trees (10–30 m). Axis 4 differentiated between moderate height forest (35–50 m) with a second cohort (5–20 m) and tall forest (>55 m) with both a second cohort (20–35 m) and bare-earth returns (<5 m). Additional axes were not included in basal area mapping because (1) they only incrementally increased the variation explained, (2) they showed little relationship with the plot-level basal area measurements, and (3) they exhibited increasingly chaotic vertical

patterns of correlations with the canopy height profile data, making interpretation of axes difficult.

*Basal area mapping*

To inform the examination of harvest edge influence on tree basal area in unharvested forest (see *Assessing edge influence*), we first developed models for predicting

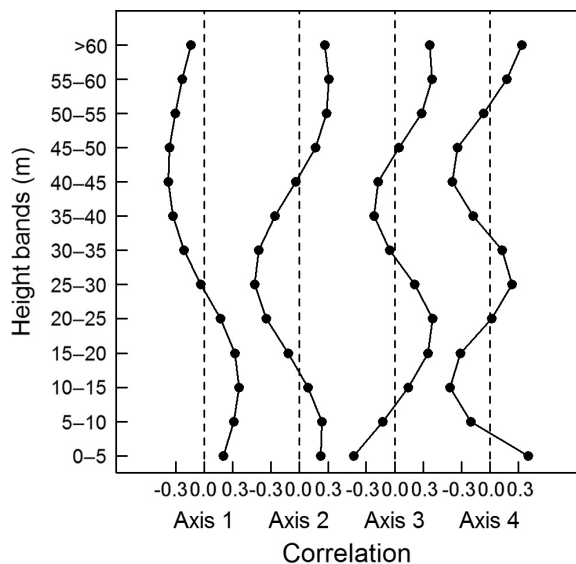


FIG. 3. Correlations between the first four axes of a principal components analysis (PCA) and the proportion of returns for an individual pixel falling into different 5-m height bands.

unharvested forest basal area based on the PCA of lidar height profiles across the study area. We used a Bayesian multivariate regression modeling procedure to explore bivariate modeling of old-growth forest basal area in the HJA. Visual inspection of the tree plot data indicated that the basal area estimates were log-normally distributed. Therefore, we log-transformed total ( $B_i$ ), upper canopy ( $U_i$ ), and lower canopy ( $L_i$ ) tree basal area for plot  $i$ . We model log upper and lower canopy basal area jointly, such that  $y_i = [U_i \ L_i] \sim N_2(\mathbf{x}_i\boldsymbol{\alpha}, \boldsymbol{\Sigma})$ , where  $\boldsymbol{\alpha}$  is an  $m \times 2$  matrix of regression coefficients,  $\mathbf{x}_i$  is a  $1 \times m$  vector of lidar principal component analysis axes (Fig. 3), quadratic, and interaction terms, and  $\boldsymbol{\Sigma}$  is a  $2 \times 2$  covariance matrix. Thus, the values of upper and lower canopy basal area depend both on the lidar measurements as well as the covariation between the two different aspects of forest structure. To compare this method with a more traditional, univariate approach, we modeled log total basal area  $B_i$  as a normally distributed random variable with mean  $x_i\beta$  and variance  $\sigma^2$ , where  $\beta$  is a  $m \times 1$  vector of regression coefficients. Models were fit with an adaptive Metropolis algorithm using JAGS (rjags package Version 4-6; Plummer 2003, 2014) within the R statistical programming environment (version 3.3.2; R Development Core Team 2016; see Metadata S1 for documentation of code). The model incorporates weak prior distributions on all parameters, representing the relatively weak prior belief in any given value of the parameter being correct and allowing the data to dominate model fitting. Priors for the regression parameters were distributed as  $N(0, 1)$ . The prior for the variance parameter for the univariate model was distributed as per  $\text{Gamma}(1,1)$ . The prior for the covariance in the bivariate model was distributed as per  $\text{Wishart}(2, \text{diag}(1))$ . Models were fit to differing combinations of main effects, quadratic effects, and interactions terms and model selection was based on posterior predictive loss (Gelfand and Ghosh 1998). Specifically, the best model was defined by the model incorporating those covariates shared by 90% of the models within 0.5 of the minimum posterior predictive loss across all models: we selected a nested model shared by 90% of the models with the lowest posterior predictive loss values (sensu Bell et al. 2014). Once the best models were selected, mean predictions were determined for each 30-m pixel from 2000 maps of total, upper canopy, and lower canopy basal area generated through 2000 realizations of parameter estimates from the Gibbs sampler. All mapping and raster manipulation was performed using the raster package (version 2.5-8; Hijmans 2016).

#### *Assessing edge influence*

The edge influence of harvests on neighboring, intact, unharvested forests is thought to decline with distance as one moves from the edge of the harvest to the core of the undisturbed forest (Chen et al. 1992, Harper et al. 2005). For all 30-m pixels in the study area, we identified the closest timber harvest and calculated the distance to

harvest edge as a gridded product (Fig. 1b). Characteristics of the timber harvest might impact the relationship between distance and basal area (i.e., the edge influence) in unharvested stands. For example, intact forests neighboring older timber harvests might have had a greater opportunity to recover and the magnitude of edge influence might increase as timber harvest sizes increase. In addition, we incorporated mean elevation of a given distance category around each harvest patch to represent the impacts of gradients in climate and soils on ecosystem structure and function in the study area.

For the purposes of assessing edge influence across the study area, we grouped 30-m pixels by 30-m harvest distance bins and harvest patch identity. Further partitioning of these distance groups by local topographic variables (i.e., aspect and slope position) did not explain additional variation in the edge influence (i.e., no interaction between aspect and distance or topographic position and distance included in best models), so these factors were excluded from the analysis described in this paper. Pixels within 15 m of harvests and roads were excluded, minimizing the chances of including measurements of harvested areas and other unnatural canopy openings. Grouping pixels based on distance helped to (1) reduce spatial heterogeneity in the data associated with fine-scale variation in canopy structure and (2) avoid the potential for identifying statistically significant and biologically insignificant effects that can be common with very large sample sizes (37,900 30-m pixels in the current study). We then calculated the mean total, upper canopy, and lower canopy basal area for each grouping.

To better account for the large amount of variation in basal areas, and thus edge influence, we analyzed the edge influence on basal area using a linear mixed-effects model with distance from harvest (m), harvest age (yr), harvest area ( $\text{m}^2$ ), mean elevation of the distance by patch grouping (m), and associated interactions as fixed effects and the harvest identity used as a random effect to account for other differences, such as ecosystem type. Total, upper canopy, and lower canopy basal areas were modeled independently (i.e., univariate models), but the model structure and evaluations were the same. The mean basal area  $z_{ij}$  for aggregate  $j$  near harvest  $k$  was modeled as  $z_{jk} = \mathbf{w}_{jk}\boldsymbol{\beta} + \gamma_k + \varepsilon_{jk}$ , where  $\mathbf{w}_{jk}$  is a  $1 \times p$  vector of covariates,  $\boldsymbol{\beta}$  is a  $p \times 1$  vector of parameter values,  $\gamma_k$  is the normally distributed harvest-specific random effect with mean 0 and variance  $\tau^2$ , and  $\varepsilon_{jk}$  is the normally distributed residual with mean 0 and variance  $\pi^2$ . Similar to the basal area mapping models, priors for the regression parameters were distributed as  $N(0, 1)$  and priors for the variance parameters ( $\pi^2$  and  $\tau^2$ ) were distributed as per  $\text{Gamma}(1,1)$ . Distance ( $D$ ), harvest age ( $A$ ), area of harvest ( $R$ ), and elevation ( $E$ ) were used as potential predictors, as well as interactions between distance and the other covariates. Interactions with distance were examined because the focus of this study was on edge influence. Random effects  $\gamma_k$  for harvest identity

(i.e., which harvest is a given area of unharvested forest nearest) may account for spatial variation in local disturbance history, such as fire, windthrow, or disease and insect attack, which might further alter forest structure. Exploratory data analysis indicated that distances needed to be square-root transformed. All covariates were rescaled to range from zero to one to aid in model convergence. Bayesian model fitting and model selection were performed in the same fashion as plot-level basal area models (see *Basal area mapping*).

## RESULTS

### *Basal area mapping*

Observed total tree basal area was well predicted, regardless of whether these predictions were based on the univariate model or the bivariate model (i.e.,  $R^2 \geq 0.44$  and  $RMSE \leq 0.27$ ; Table 1). Models for total and upper canopy tree basal area were similar and incorporated the first four PCA axes for canopy height profile while the model for lower canopy tree basal area incorporated only the second and third axes (Appendix S1). The basal area models indicated that high total and upper canopy basal area predictions were associated with the lidar returns arising from taller trees (>30 m) while high lower canopy basal area predictions were associated with the returns arising from the secondary canopy (10–35 m). Total and upper canopy basal areas were greatest in the eastern portion of the study area (Fig. 4 and Appendix S2: Fig. S1) associated with greater elevations (Fig. 1a) and forest canopy heights (Fig. 2). No clear geographic trend in lower canopy basal area was apparent (Appendix S2: Fig. S2). Still, these maps highlight a high degree of spatial variation in forest basal area across unharvested forest in the HJA that is itself related to vertical variation in forest structure measured directly by lidar data.

### *Assessing edge influence*

Linear mixed effects models with distance and elevation performed best for total, upper canopy, and lower

TABLE 1. Lidar-based basal area model performance in unharvested forests ( $n = 102$ ) based on the coefficient of determination ( $R^2$ ) and the root mean square error (RMSE).

Response variable	$R^2$	RMSE (ln[m <sup>2</sup> /ha])
Bivariate model		
Lower canopy basal area	0.09	0.47
Upper canopy basal area	0.48	0.33
Total basal area	0.45	0.27
Univariate model		
Total basal area	0.44	0.28

*Note:* Best models were selected as those where all predictor variables were included in the 10 models with the lowest posterior predictive losses.

canopy basal area (Table 2), with additional variation roughly evenly split between random effects and the model residuals (Table 3). Unsurprisingly, mean basal areas (i.e., intercepts from models) were greatest for total, followed by upper and lower canopy basal area. Positive effects of the square root distance  $D^{0.5}$  indicated that upper canopy, lower canopy, and total basal area increased with distance from harvest edge. Interactions between distance and other covariates were included in all models (Table 3). Edge influence decreased with elevation for total, upper canopy, and lower canopy basal area (Figs. 5a–c), indicating elevated basal area near edges at low elevations and reduced basal area at high elevations. Edge influence increased with harvest area for total and upper canopy basal area (Figs. 5d–f), indicating reduced basal area near edges for small harvests and no effect for large harvests. Edge influence was impacted by harvest age for upper canopy trees only and the effect did not differ from zero. Such patterns imply that edge influence across the study area was mediated by additional biophysical and historical gradients.

Given that harvest age, harvest area, and elevation of unharvested forest with the study area are not equally and evenly distributed, we used the linear mixed effects models to predict landscape edge influences across the study area. After weighting predicted effects of edges by the areas of patches, mean landscape basal area was reduced by 6.3% between 15 and 45 m of harvests (10.6% of the unharvested forest), 4.8% between 45 and 75 m (11.0% of the unharvested forest), and 1.0% at distances greater than 75 m, with upper canopy basal area following a similar pattern with slightly greater magnitude of edge influence (78.4% of the unharvested forest; Fig. 6). Mean upper canopy basal area was reduced by 6.8%, 5.3%, and 1.0% across the three distances (15–45 m, 45–75 m, >75 m, respectively) from the harvest edge (Fig. 6). While lower canopy basal area accounted for a small portion of total basal area (Appendix S1), mean lower canopy basal area was reduced by 3.9%, 3.0%, and 0.7% across the three distances (15–45 m, 45–75 m, >75 m, respectively) from the harvest edge (Fig. 6). Variation in the edge influence on lower canopy basal area was substantial. This high variation was due to the interaction between elevation and distance (Table 3), resulting in a positive edge influence at low elevations (<800 m) and a negative edge influence at moderate to high elevations (>800 m; Fig. 5c). Similar patterns were observed for total and upper canopy basal area (Fig. 5a, b), but greater uncertainty in parameter estimates reduced its impact on variation observed across the landscape (Fig. 6).

## DISCUSSION

Our study indicates that the edge influence of past clearcutting of old growth on current structure of remaining old-growth forest is widespread and persistent. Roughly 60% of the forest between 400 and 1,100 m elevation in the HJA remains uncut, but a substantial

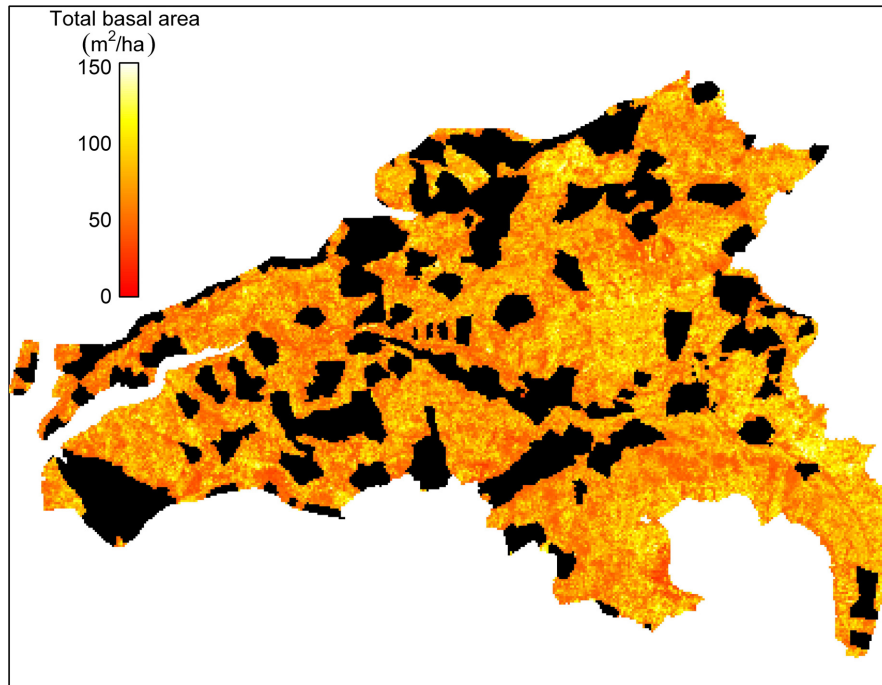


FIG. 4. Mean predicted total tree basal area (lower canopy + upper canopy trees) for the study area. Black areas represent timber harvests and were not modeled (Fig. 1b). [Color figure can be viewed at wileyonlinelibrary.com]

TABLE 2. Model selection to understand impacts of distance, harvest characteristics (age and area), and environment (elevation and aspect) based on posterior predictive loss (PPL).

$\Delta$ PPL	Model
Lower canopy basal area	
0	$D^{0.5} + R + E + D^{0.5} \times E$
0.6	$D^{0.5} + E + D^{0.5} \times E$
2.8	$D^{0.5} + R + E + D^{0.5} \times R + D^{0.5} \times E$
3.8	$D^{0.5} + A + E + D^{0.5} \times A + D^{0.5} \times E$
Upper canopy basal area	
0	$D^{0.5} + A + R + E + D^{0.5} \times A + D^{0.5} \times R + D^{0.5} \times E$
58.5	$D^{0.5} + R + E + D^{0.5} \times R + D^{0.5} \times E$
68.6	$D^{0.5} + A + R + E + D^{0.5} \times A + D^{0.5} \times R$
214.7	$D^{0.5} + A + R + E + D^{0.5} \times R$
Total basal area	
0	$D^{0.5} + A + R + E + D^{0.5} \times R + D^{0.5} \times E$
110.1	$D^{0.5} + A + R + E + D^{0.5} \times A + D^{0.5} \times R + D^{0.5} \times E$
173.5	$D^{0.5} + R + E + D^{0.5} \times R + D^{0.5} \times E$
413.6	$D^{0.5} + A + R + D^{0.5} \times A + D^{0.5} \times R$

Notes: *D*, distance; *A*, harvest age; *R*, area of harvest; *E*, elevation. Best models were defined by those that minimized PPL (i.e.,  $\Delta$ PPL = 0 for best model). Because the focus of this study was on edge influence, interactions not including distance were ignored.

percentage of that uncut landscape appears to have reduced basal area through indirect effects of historical timber harvests (Fig. 6). Forests within 75 m of harvest edges have 4% to 6% less live basal area than forest interiors. At higher elevations, these reductions approached 10%. The distance of edge influence in this study is similar to previous research within our study area focused on a 96-ha harvest unit (50–100 m, approximately 1–2 tree

heights), where the distribution of snags indicated elevated mortality (Chen et al. 1992). The greater mortality and associated basal area declines are most likely due to greater exposure to wind and storm damage and possibly some partial harvest (usually done to remove “hazard” trees) outside the cutting units that occurred at the time of the logging. In contrast to this previous work, which focused on a few cutting units, our landscape-scale

TABLE 3. Posterior mean parameter estimates for landscape-level edge influence analysis of lidar-based basal area predictions.

Parameter	Basal area models for edge influence		
	Lower canopy	Upper canopy	Total
Intercept	11.6 (0.5)†	54.3 (2.9)†	67.9 (3.1)†
$D^{0.5}$	0.5 (0.1)†	4.9 (0.7)†	5.4 (0.7)†
$E$	-1.7 (0.3)†*	13.3 (2.4)†	11.7 (2.6)†
$A$		-3.3 (2.9)	-2.0 (3.0)
$R$	-0.8 (0.7)	-2.6 (4.2)	-5.4 (4.4)
$D^{0.5} \times A$		-3.9 (3.1)	
$D^{0.5} \times R$		-10.6 (4.8)†	-12.1 (5.0)†
$D^{0.5} \times E$	1.9 (0.4)†	2.3 (2.9)	5.5 (2.9)
$\sigma$	0.9	6.5	6.8
$\tau$	1.1	7.4	7.5

Notes:  $D$ , distance;  $A$ , harvest age;  $R$ , area of harvest;  $E$ , elevation;  $\sigma$ , standard deviation of the residuals;  $\tau$ , standard deviation of the harvest-level random effects. Values are means with SD in parentheses.

† Indicate that 95% credible intervals do not include zero.

assessment indicates the extent the timber harvesting edge influence across a 700-m elevational gradient in the western Cascade Mountains. Within this region and elevational band, most federal forests are now managed to conserve and grow as multi-storied old growth forests under the Northwest Forest Plan (Davis et al. 2015). The HJA has probably experienced less clear cutting than

areas of general federal forest, consequently the proportion of the unlogged forest landscape outside our study area experiencing reductions in live tree basal area associated with historical timber harvest edges is probably greater.

The ecological consequences of basal area reductions over 20% of the unharvested landscape are not well understood. Areas of lower basal area of upper canopy trees are part of the heterogeneity of canopies and gaps in old-growth forests in this area (Cohen et al. 1990, Spies et al. 1990). However, edge-associated areas of lower basal area may fall below the normal range in older forests and could reduce habitat quality of species such as the Northern Spotted Owl whose habitat is associated with density of large conifers and tree height (Ackers et al. 2015). The widespread nature of the edge influence also suggests that carbon sequestration in old-growth forests has been reduced somewhat by proximity to harvest edges. On the other hand, an increase in standing dead and fallen trees could benefit species such as pileated woodpeckers that use dead wood for habitat (Mellen et al. 1992), and decreases in tree cover could increase diversity of understory plant communities in dense conifer forests (Fahey et al. 2008). Microclimate is likely heavily altered by harvest edge influence (Chen et al. 1999, Schmidt et al. 2017), potentially minimizing the capacity of old-growth forest structure to buffer forest understories against climate change (sensu Frey et al. 2016). Such changes in microclimate may also impact epiphyte communities distributed throughout forest canopies (van Rooyen et al. 2011). In short, the composition, structure, and function of unharvested forests are likely to differ dramatically in these forest edges and we do not know how long it will take for recovery to occur.

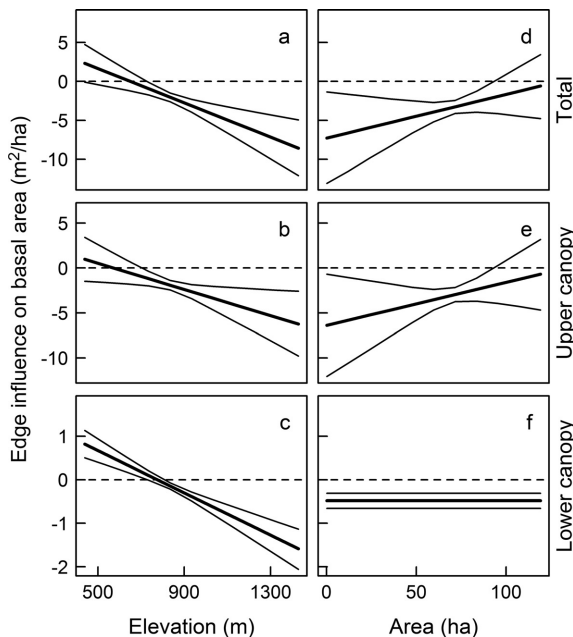


FIG. 5. Influence of (a–c) elevation and (d–f) harvest area on the edge influence for basal area from (a, d) all trees, (b, e) upper canopy trees, and (c, f) lower canopy trees as measured by the difference between predicted basal areas in edge (e.g., 15–45 m from harvest edge) and core (>195 m from harvest edge) portions of the old-growth forest. Because  $D^{0.5} \times A$  did not differ from zero for lower canopy, upper canopy, or all tree models (Table 3), we do not present that interaction here.

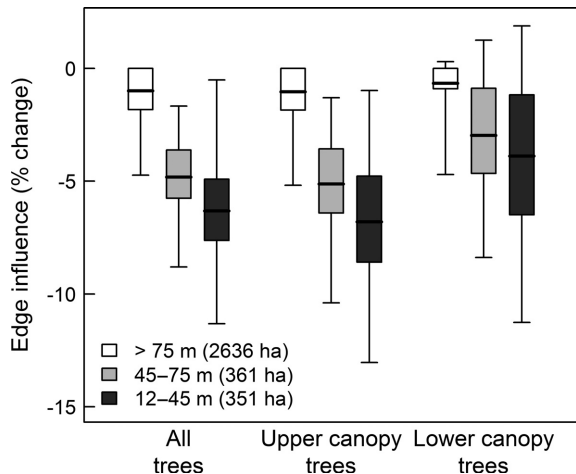


FIG. 6. Edge influence on basal area (percentage change in basal area) weighted by forest areas for all trees, lower canopy trees, and upper canopy trees at differing distance from the harvest edge. The figure represents the mean (thick horizontal bar), the 25% to 75% percentile interval (box), and 2.5% to 97.5% percentile interval (whiskers) of edge influences for a given distance category across all harvest patches.

We hypothesized that size and age of harvest units might modify edge influence on basal area, based on the assumption that larger harvests might have larger impacts on the landscape and that greater time since harvest offers greater opportunities for recovery in basal area (i.e., recruitment and growth). Surprisingly, we found greater negative edge influence on total and upper canopy basal area around small, rather than large, timber harvests and no effect on lower canopy basal area (Fig. 5), despite the presence of harvests ranging two orders of magnitude in size (0.2–119.0 ha). Elevated atmospheric turbulence associated with harvests may be sufficient to expose neighboring trees to elevated risk of windthrow even in small harvests, which in turn can increase the likelihood of additional windthrow in Pacific Northwest forests (i.e., windthrow begets windthrow; Sinton et al. 2000, Harcombe et al. 2004). However, this does not explain why edge influence would disappear as harvest size increases. Additionally, the relatively large ratio of standard deviation to mean parameter estimate for the  $D^{0.5} \times R$  interaction effects (0.37–0.40) indicate high uncertainty in this effect. We found little or no harvest age interactions with distance (Table 3), though harvest ages mostly ranged from 13 to 60 yr. The lack of strong age effects could be because we lacked harvests that were either (1) young (<13 yr old) where windthrow hazard might remain high and be ongoing (Ruel 1995) or (2) old (>60 yr) where recovery processes might be more advanced. While there was little age effect, we did observe a shift from a positive edge influence (higher basal area near edge) to a negative edge influence (lower basal area near edge) in lower canopy trees as elevation increased (Fig. 5), indicating that trees in the lower canopy might be responding positively to overstory mortality in warmer, more productive environments. A similar pattern was observed for upper canopy and all trees, though the shift was from no effect to a negative edge influence with elevation. If recovery rates are energy limited (i.e., faster recovery in warmer ecosystems), age effects may be confounded with temperature effects, as the oldest and largest harvests in the landscape tended to be at lower elevations (Pearson correlation between harvest age and elevation =  $-0.26$ ).

Vertical and horizontal variation in vegetation structure of old-growth forests may also impact edge influence. For example, patch contrast (i.e., difference in composition, structure, and function between unharvested and harvested forests) can drive edge influence on forest structure and dynamics (Harper et al. 2005, Esseen et al. 2016). We could not easily examine these factors directly because canopy height enters the modeling of basal area, making inferences on how these factors impact basal area at the landscape scale tautological. An interesting alternative would be to leverage physical models of air turbulence as a predictor variable, the presumed driver of windthrow related mortality along clearcut boundaries (Ruel 1995), which

could encapsulate the various risk factors associated with wind-related edge influence of past harvests.

In addition to the ecological differences between upper and lower canopy tree responses, our partitioning of canopy basal area highlights the importance of recognizing the limits of lidar when mapping forest structure. Greater predictive performance for upper compared to lower canopy basal area (Table 1) reflects the fact that aerial lidar data provide extensive information about trees with exposed canopies, but the richness of the information declines as we examine obscured components (Latifi et al. 2016), such as suppressed and intermediate canopy trees. Predictive performance for total basal area based on our bivariate method (upper canopy + lower canopy) did not differ from traditional univariate approaches (Table 1), raising the question: why go through the trouble to separate out the lower canopy? In situations where only the largest, canopy dominant trees are important, this partitioning of basal area may be of little practical use, especially given the uncertainties in lower canopy basal area predictions ( $R^2 = 0.09$ ). However, ignoring the structural complexity in both the landscape and the lidar data risks missing a key aspect of landscape structure. Despite striking similarities between the two methodologies in terms of coefficients of determination, 17% and 4% of the predicted 30-m pixels differ by more than 5 and 10  $m^2/ha$  basal area, respectively. These differences arose because (1) upper and lower canopy basal area regression functions differed substantially and (2) covariance between the two basal area components was not different from zero (Appendix S1).

The study provides yet another example of how the legacies of land use activities can persist in natural and semi-natural ecosystems for many decades and potentially longer after the cessation of the activity or event (Foster et al. 2003). These land use legacies reach into neighboring stands, diffusely altering landscape structure (Harper et al. 2005). The effects of human activities can be both dramatic, e.g., replacing an old growth forest with a plantation, and subtle, as we have demonstrated here for edge influence on forest structure. Subtle human impacts can be important, especially if they are widespread and persistent, but they are generally not well studied (McDonnell and Pickett 2012). This research examines just such a subtle impact of human activity and highlights the connectivity within forest landscapes of the Cascade Mountains of Western Oregon. Our result show that changes in old-growth forest ecosystems can be caused by management in a neighboring forest stand and persist for decades, implying that spatial variation in management, within or across forest ownership boundaries, is not as simple as delineating where and when harvests occurred. Such issues may contribute to conflicts between ownerships with drastically differing management objectives and highlights the need for landscape-level science and planning. It remains to be seen how much longer these structural effects can be detected or how much other components of the ecosystem track the changes in forest structure that we observed here.

## ACKNOWLEDGMENTS

We thank Keith Olsen, Matt Gregory, and Zhiqiang Yang for support in acquiring remote sensing and geospatial data layers used in this study. We also thank George McFadden for his support of forest mapping and change research represented by this project. We thank the H. J. Andrews Experimental Forest, the H. J. Andrews LTER (NSF DEB-1440409), Oregon State University, and the Pacific Northwest Research Station for providing the data and financial support. Any use of trade, product, or firm names is for descriptive purposes only and does not imply endorsement by the US Government.

## LITERATURE CITED

- Ackers, S. H., R. J. Davis, K. A. Olsen, and K. M. Dugger. 2015. The evolution of mapping habitat for northern spotted owls (*Strix occidentalis caurina*): a comparison of photo-interpreted, Landsat-based, and lidar-based habitat maps. *Remote Sensing of Environment* 156:361–373.
- Andersen, H.-E., S. E. Reutebuch, and R. J. McGaughey. 2014. A rigorous assessment of tree height measurements obtained using airborne lidar and conventional field methods. *Canadian Journal of Remote Sensing* 32:355–366.
- Bell, D. M., J. B. Bradford, and W. K. Lauenroth. 2014. Forest stand structure, productivity, and age mediate climatic effects on aspen decline. *Ecology* 95:2040–2046.
- Canham, C. D. 1988. Growth and canopy architecture of shade-tolerant trees: response to canopy gaps. *Ecology* 69:786–795.
- Chen, J., J. F. Franklin, and T. A. Spies. 1992. Vegetation responses to edge environments in old-growth Douglas-fir forests. *Ecological Applications* 2:387–396.
- Chen, J., J. F. Franklin, and T. A. Spies. 1993. Contrasting microclimates among clearcut, edge, and interior of old-growth Douglas-fir forest. *Agricultural and Forest Meteorology* 63:219–237.
- Chen, J., J. F. Franklin, and T. A. Spies. 1995. Growing-season microclimatic gradients from clearcut edges into old-growth Douglas-fir forests. *Ecological Applications* 5:74–86.
- Chen, J. Q., S. C. Saunders, T. R. Crow, R. J. Naiman, K. D. Brosofske, G. D. Mroz, B. L. Brookshire, and J. F. Franklin. 1999. Microclimate in forest ecosystem and landscape ecology - Variations in local climate can be used to monitor and compare the effects of different management regimes. *BioScience* 49:288–297.
- Clark, J. S., B. D. Soltoff, A. S. Powell, and Q. D. Read. 2012. Evidence from individual inference for high-dimensional coexistence: long-term experiments on recruitment response. *PLoS ONE* 7:e30050.
- Cohen, W. B., T. A. Spies, and G. A. Bradshaw. 1990. Semivariograms of digital imagery for analysis of conifer canopy structure. *Remote Sensing of Environment* 34:167–178.
- Davis, R. J., J. L. Ohmann, R. E. Kennedy, W. B. Cohen, M. J. Gregory, Z. Yang, H. M. Roberts, A. N. Gray, and T. A. Spies. 2015. Northwest Forest Plan—the first 20 years (1994–2013): status and trends of late-successional and old-growth forests. General Technical Report PNW-GTR-911. U.S. Department of Agriculture, Forest Service, Pacific Northwest Research Station, Portland, OR. 112 p.
- Esseen, P.-A., A. Hedström Ringvall, K. A. Harper, P. Christensen, and J. Svensson. 2016. Factors driving structure of natural and anthropogenic forest edges from temperate to boreal ecosystems. *Journal of Vegetation Science* 27:482–492.
- Fahey, R. T., and K. J. Puettmann. 2008. Patterns in spatial extent of gap influence on understory plant communities. *Forest Ecology and Management* 255:2801–2810.
- Finley, A. O., S. Banerjee, B. D. Cook, and J. B. Bradford. 2013. Hierarchical Bayesian spatial models for predicting multiple forest variables using waveform LiDAR, hyperspectral imagery, and large inventory datasets. *International Journal of Applied Earth Observation and Geoinformation* 22:147–160.
- Foster, D., F. Swanson, J. Aber, I. Burke, N. Brokaw, D. Tilman, and A. Knapp. 2003. The importance of land-use legacies to ecology and conservation. *BioScience* 53:77–88.
- Franklin, J. F., et al. 2002. Disturbances and structural development of natural forest ecosystems with silvicultural implications, using Douglas-fir forests as an example. *Forest Ecology and Management* 155:399–423.
- Frazier, G. W., S. Magnussen, M. A. Wulder, and K. O. Niemann. 2011. Simulated impact of sample plot size and co-registration error on the accuracy and uncertainty of LiDAR-derived estimates of forest stand biomass. *Remote Sensing of Environment* 115:636–649.
- Frey, S. J. K., A. S. Hadley, S. L. Johnson, M. Schulze, J. A. Jones, and M. G. Betts. 2016. Spatial models reveal the microclimatic buffering capacity of old-growth forests. *Science Advances* 2:e1501392.
- Gelfand, A. E., and S. K. Ghosh. 1998. Model choice: a minimum posterior predictive loss approach. *Biometrika* 85:1–11.
- Gray, A. N., T. A. Spies, and M. J. Easter. 2002. Microclimatic and soil moisture responses to gap formation in coastal Douglas-fir forests. *Canadian Journal of Forest Research* 32:332–343.
- Harcombe, P. A., S. E. Greene, M. G. Kramer, S. A. Acker, T. A. Spies, and T. Valentine. 2004. The influence of fire and windthrow dynamics on a coastal spruce-hemlock forest in Oregon, USA, based on aerial photographs spanning 40 years. *Forest Ecology and Management* 194:71–82.
- Harper, K. A., S. E. Macdonald, P. J. Burton, J. Chen, K. D. Brosofske, S. C. Saunders, E. S. Euskirchen, D. Roberts, M. S. Jaiteh, and P. A. Esseen. 2005. Edge influence on forest structure and composition in fragmented landscapes. *Conservation Biology* 19:768–782.
- Harper, K. A., et al. 2015. Edge influence on vegetation at natural and anthropogenic edges of boreal forests in Canada and Fennoscandia. *Journal of Ecology* 103:550–562.
- Hijmans, R. J. 2016. raster: Geographic data analysis and modeling. R package version 2.5-8. <https://CRAN.R-project.org/package=raster>
- Huggard, D. J., W. Klenner, and A. Vyse. 1999. Windthrow following four harvest treatments in an Engelmann spruce - subalpine fir forest in southern interior British Columbia, Canada. *Canadian Journal of Forest Research* 29:1547–1556.
- Hurlbert, S. 1984. Pseudoreplication and the design of ecological field experiments. *Ecological Monographs* 54:187–211.
- Kennedy, R. E., Z. Yang, W. B. Cohen, E. Pfaff, J. Braaten, and P. Nelson. 2012. Spatial and temporal patterns of forest disturbance and regrowth within the area of the Northwest Forest Plan. *Remote Sensing of Environment* 122:117–133.
- Latifi, H., M. Heurich, F. Hartig, J. Müller, P. Krzystek, H. Jehl, and S. Dech. 2016. Estimating over- and understorey canopy density of temperate mixed stands by airborne LiDAR data. *Forestry* 89:69–81.
- Lefsky, M. A., W. B. Cohen, S. A. Acker, G. G. Parker, T. A. Spies, and D. Harding. 1999. Lidar remote sensing of the canopy structure and biophysical properties of Douglas-fir western hemlock forests. *Remote Sensing of Environment* 70:339–361.
- Luoma, J. R. 2006. The hidden forest: the biogeography of an ecosystem. Oregon State University Press, Corvallis, Oregon, USA.

- McDonnell, M. J., and S. T. A. Pickett, editors. 2012. *Humans as components of ecosystems: the ecology of subtle human effects and populated areas*. Springer Science & Business Media, New York, New York, USA.
- Mellen, T. K., E. C. Meslow, and R. W. Mannan. 1992. Summertime home range and habitat use of pileated woodpeckers in western Oregon. *Journal of Wildlife Management* 56:96–103.
- Oksanen, L. 2001. Logic of experiments in ecology: is pseudoreplication a pseudoissue? *Oikos* 94:27–38.
- Plummer, M. 2003. JAGS: A program for analysis of Bayesian graphical models using Gibbs sampling. Proceedings of the 3rd International Workshop on Distributed Statistical Computing (DSC 2003). March:20–22.
- Plummer, M. 2014. rjags: Bayesian graphical models using MCMC. R package version 4-6. <https://CRAN.R-project.org/package=rjags>
- R Development Core Team, R. 2016. R: a language and environment for statistical computing. R Foundation for Statistical Computing, Vienna, Austria. <https://www.R-project.org/>
- Ruel, J. 1995. Understanding windthrow: silvicultural implications. *Forestry Chronicle* 71:434–445.
- Schmidt, M., H. Jochheim, K. C. Kersebaum, G. Lischeid and C. Nendel. 2017. Gradients of microclimate, carbon and nitrogen in transition zones of fragmented landscapes—a review. *Agricultural and Forest Meteorology* 232:659–671.
- Seidl, R., T. A. Spies, W. Rammer, E. A. Steel, R. J. Pabst, and K. Olsen. 2012. Multi-scale drivers of spatial variation in old-growth forest carbon density disentangled with lidar and an individual-based landscape model. *Ecosystems* 15:1321–1335.
- Sinton, D. S., J. A. Jones, J. L. Ohmann, and F. J. Swanson. 2000. Windthrow disturbance, forest composition, and structure in the Bull Run basin, Oregon. *Ecology* 81:2539–2556.
- Spies, T. A., J. F. Franklin, and M. Klopsch. 1990. Canopy gaps in Douglas-fir forests of the Cascade Mountains. *Canadian Journal of Forest Research* 20:649–658.
- Spies, T. A., W. J. Ripple, and G. A. Bradshaw. 1994. Dynamics and pattern of a managed coniferous forest landscape in Oregon. *Ecological Applications* 4:555–568.
- Turner, M. G. 2010. Disturbance and landscape dynamics in a changing world. *Ecology* 91:2833–2849.
- van Rooyen, J. C., J. M. Malt, and D. B. Lank. 2011. Relating microclimate to epiphyte availability: edge effects on nesting habitat availability for the marbled murrelet. *Northwest Science* 85:549–561.
- Wing, B. M., M. W. Ritchie, K. Boston, W. B. Cohen, and M. J. Olsen. 2014. Individual snag detection using neighborhood attribute filtered airborne lidar data. *Remote Sensing of Environment* 163:165–179.
- Zald, H. S. J., T. A. Spies, R. Seidl, R. J. Pabst, K. A. Olsen, and E. A. Steel. 2016. Complex mountain terrain and disturbance history drive variation in forest aboveground live carbon density in the western Oregon Cascades, USA. *Forest Ecology and Management* 366:193–207.

## SUPPORTING INFORMATION

Additional supporting information may be found online at: <http://onlinelibrary.wiley.com/doi/10.1002/eap.1560/full>

## DATA AVAILABILITY

Data associated with this paper are available online. Lidar data: <http://dx.doi.org/10.6073/pasta/c47128d6c63dff39ee48604ecc6fabfc>

Plot data: <http://dx.doi.org/10.6073/pasta/2315afa15ad0a2317b49565da6258c47>